# Effect of Modulated Robotically Rendered Viscosity During Hand Grasping on Brain Activity

Chenchen Qi
*Faculty of Mechanical Engineering*
*Delft University of Technology*
Delft, The Netherlands
Qi.Chenchen@outlook.com

Alexandre L. Ratschat
*Delft University of Technology*
Delft, The Netherlands
*Erasmus MC*
Rotterdam, The Netherlands
A.L.Ratschat@tudelft.nl

Mark van de Ruit
*Faculty of Mechanical Engineering*
*Delft University of Technology*
Delft, The Netherlands
M.L.vandeRuit-1@tudelft.nl

Laura Marchal-Crespo
*Delft University of Technology*
Delft, The Netherlands
*Erasmus MC*
Rotterdam, The Netherlands
L.MarchalCrespo@tudelft.nl

2025 IEEE World Haptics Conference (WHC) | 979-8-3315-3353-3/25/$31.00 ©2025 IEEE | DOI: 10.1109/WHC64065.2025.11123209

***Abstract*—Robotic rehabilitation systems may benefit from haptic rendering to provide sensorimotor training to patients with acquired brain injuries. Haptic rendering usually involves modulating stiffness and viscosity to simulate real-world hand-object interactions. Yet, the effect of rendering different viscosities on brain activity remains mainly unexplored. To fill this gap, we ran an experiment with twelve unimpaired participants who were asked to grasp and release virtual liquid dispensers whose stiffness and viscosity were rendered using a haptic hand rehabilitation robot. All liquid dispensers had identical wall stiffness but contained liquids of three different viscosities. We also incorporated control conditions without viscosity and stiffness rendering, involving both passive and active grasping movements. Electroencephalography data were recorded during the experiment. We found stronger ipsilateral somatosensory mu and beta event-related desynchronization during movements with viscosity and stiffness rendering compared to the control conditions, while different viscosity levels did not result in significant variations. Furthermore, no significant electroencephalography activity differences were found between control conditions. These findings indicate that while viscosity and stiffness rendering strengthens brain activity, modulating viscosity levels does not significantly affect this response. This insight may contribute to the design of rehabilitation games by informing the choice of viscosity rendering parameters.**

***Index Terms*—Haptic rendering, viscosity rendering, EEG, proprioception, neurorehabilitation**

## I. Introduction

Using robots for neurorehabilitation is attractive because they provide controllable, repeatable, and intensive training while ensuring user safety [1], [2]. Robots are generally used to physically assist the user's limbs during movement training, the so-called robotic assistance, thus alleviating physical strain on therapists [3]. While promising, robotic training has been shown to limit the recovery of functional movements needed to perform activities of daily living (ADL) [4], crucial to regain independence. Many ADLs, such as carrying a cup of coffee, require physical interaction with objects with complex dynamics. Yet, this sensory information is usually missing during robotic interventions [5]. Current solutions try to compensate for the lack of somatosensory information by relying on visual information from abstract visualizations on computer screens. The result is that visuo-haptic incongruencies worsen the persisting gap between the complex dynamics of real-life objects and the simplified (or null) dynamics of virtual objects [6].

Thus, a promising approach is to provide somatosensory information from hand-object interaction using haptic rendering, i.e., simulating the interaction forces of tangible virtual objects to participants according to their dynamic models involving virtual springs and viscosity [7]–[9]. Haptic rehabilitation systems that provide enriched sensory experiences to enhance motor learning are rapidly developing [9], [10]. Nonetheless, the effects of augmented somatosensory feedback from haptic rehabilitation systems—such as modifications to the dynamic properties of objects used in ADL—on the central nervous system activity and, thereby, the ability to enhance motor learning, remain unclear.

One study specifically investigated the modulating effect of spring-like interaction tasks on brain activity. The authors reported increased somatosensory activity during tasks compared to the rest period [11]. Other studies have used fixed loads to investigate the modulating effects of forces during sensorimotor tasks on electroencephalography (EEG) activity. They showed that while the presence of the load enhances the sensorimotor cortical activity, varying the magnitude of the load does not significantly modulate the EEG activities in the mu, beta, and gamma bands [12]–[14]. However, higher force requirements specifically enhance contralateral mu band EEG activity in the somatosensory cortex, reflected by increased event-related desynchronization (mu-ERD) [15]. To our knowledge, the

This study was funded by the Dutch Research Council (NWO, VIDI Grant Nr. 18934).

effect of different levels of viscosity on brain activity remains unstudied. This is quite a limitation, as viscous fields have been proposed as an effective method to provide participants with an enriched sensorimotor experience of the trained task that can challenge the motor system, reinforcing the neural pathways that govern movement [16]–[18].

To address this limitation, we aimed to answer the following research question: Does viscosity rendering during functional tasks modulate activity in the somatosensory cortex? To answer this question, we investigated how viscosity rendering during grasping movements influences the EEG activity in the somatosensory cortex. We conducted a within-subject study with 12 unimpaired participants in which they squeezed a virtual fluid-filled liquid dispenser with fixed wall stiffness and varying fluid viscosities. The experiment included five conditions: two control conditions with robotically-guided passive movement and active movement without haptic rendering, and three active movement conditions with haptic rendering and different viscosity levels. We collected EEG, kinematic, and performance data, along with questionnaires including the raw NASA-Task Load Index (raw-TLX) [19] and additional questions about perceived haptic rendering levels. The raw-TLX was included since a high workload may affect performance and proprioceptive sensation [20], [21].

We hypothesized that active movement conditions with haptic rendering would induce greater activity in the somatosensory cortex, reflected in increased mu-ERD and beta-ERD, compared to the control conditions without haptic rendering. Additionally, we expected that higher viscosity would result in further increases in mu-ERD and beta-ERD.

## II. Methods

### A. Participants

Twelve unimpaired adults (six male, six female) aged 22 to 29 (median age 25) from TU Delft participated in the study. All participants self-reported being right-handed, healthy, and free of proprioceptive deficits. The study was approved by the TU Delft Human Research Ethics Committee (HREC, Application ID 4428). All participants gave written informed consent and received no compensation.

### B. Experimental Setup

We employed the PRIDE haptic device developed by Rätz et al. for upper-limb rehabilitation (Fig. 1A). PRIDE is a one Degree-of-Freedom (DoF) device capable of fine haptic rendering and supporting physiological full flexion/extension of collective fingers, from the index to the little finger [22]. The device was controlled in Python 3.9.19 (Python Software Foundation, United States) and ran at $500\,\mathrm{Hz}$ [23], ensuring high-quality haptic rendering [24], [25].

The viscosity exploration task was designed to provide the experience of squeezing a liquid dispenser with different liquids inside. The virtual environment was built in Unity 2020.3.25f1 (Unity Technologies, United States) and ran at $200\,\mathrm{Hz}$.

EEG recordings were acquired by asaLab 4.9.4 (ANT Neuro, the Netherlands) with WaveGuard caps containing 128 electrodes (ANT Neuro, the Netherlands) and TMSi Refa_Ext amplifier (TMSi, the Netherlands), using an average reference and sampling at $2048\,\mathrm{Hz}$. The EEG amplifier was connected to a trigger box developed using an Arduino UNO microcontroller board (Arduino, Italy). The trigger box could receive commands from the exploration task in Unity and then send pulses to the corresponding trigger channels of the EEG amplifier.

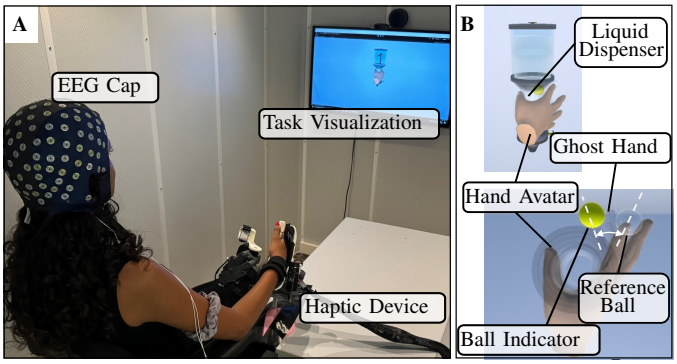


Fig. 1. Overview of the experimental setup. (A) Participants were sitting in a soundproof cabin during the experiment, wearing an EEG cap and using the haptic device while looking at the task visualization. (B) Front and top view of the task visualization. The solid hand avatar followed the movements of the participant's fingers. The semi-transparent "ghost hand" provided a visual guide for participants to move at the desired pace. The indicator sphere attached to the ghost hand indicates the magnitude of the tracking error (yellow for a large error). The two white dotted lines display the angular error between actual and desired angular position, which is $45°$ here. Participants visualized the task from a first-person perspective, as depicted on the left.

### C. Experiment Protocol

Participants were seated in a soundproof cabin with earplugs to minimize noise. The correctly sized EEG cap was fitted, with the ground electrode placed on the right mastoid. Electrode gel was applied to reduce impedance below $5\,\mathrm{k}\Omega$.

During the experiment, participants sat in a comfortable chair with wheels locked in front of a screen on the front wall. The haptic device was securely attached to a table in front of them, at a height that allowed participants to grasp it comfortably, as shown in Fig. 1A. An appropriately sized handle (four sizes available) was installed in the haptic device for each participant based on their hand measurements. To simplify the task, the thumb submodule was not used in this study, and the thumb rested on the handle during the experiment.

Participants were instructed to open and close their hands, i.e., extending and flexing their fingers from $45°$ (finger extension) to $145°$ (finger flexion), to squeeze a virtual liquid dispenser. Here, the finger flexion/extension angle was defined as the angle between the distal phalanx and the metacarpal of the index finger. A hand avatar that moved following the movements of participants' real hands was visualized on the screen (Fig. 1B). The virtual liquid dispenser was cylindrical and was located in the palm of the avatar's hand.

Participants were asked to complete one hand opening and closing movement every two seconds. To guide them in performing the task at the predefined trace and velocity, a semitransparent "ghost hand" avatar opened and closed at

the desired velocity, providing visual guidance. The reference finger flexion/extension angle followed a sinusoidal curve $y(t) = -50\cos(\pi t) + 95$, where $t$ is the elapsed time within a trial. A semi-transparent reference sphere was attached to the tip of the avatar's index finger, and a solid sphere was attached to the ghost hand. Participants were instructed to move their hands in sync with the solid sphere indicator and the ghost hand, ensuring they always overlapped. The solid sphere changed colors to provide real-time feedback based on the tracking error, i.e., the angular difference between the respective spheres (green: acceptable, yellow: caution, red: warning). To protect the haptic device from damage, virtual soft stops located at $10^\circ$ and $160^\circ$ were added at both ends of the device's maximum range of motion (from $0^\circ$ to $180^\circ$).

The experiment included five different conditions: three viscosity conditions and two control conditions. The appearance of the liquids in the virtual environment remained the same for all conditions to minimize the visual effect on sensation. During the viscosity conditions, the liquid dispenser was assigned a constant wall stiffness of K = $4\,\mathrm{N/m}$. The fluid in the liquid dispenser was randomly assigned one of three viscosities, which were approximated using damping coefficients (B): $\mathrm{B}_1$ = $20\,\mathrm{N\,s/m}$, $\mathrm{B}_2$ = $50\,\mathrm{N\,s/m}$, or $\mathrm{B}_3$ = $90\,\mathrm{N\,s/m}$. We determined these viscosity levels through a pilot experiment to ensure distinguishable differences and utilize the haptic device's effective force output range. We also included two control conditions: active and passive. During these conditions, the stiffness and viscosity of the liquid dispenser were set to 0. In the passive session, a Proportional-Derivative (PD) controller ($\mathrm{K_p}$ = $0.08\,\mathrm{N/^\circ}$, $\mathrm{K_d}$ = $1\,\mathrm{N\,s/^\circ}$) passively moved the participants' fingers to follow the reference trace. During the active session, participants were asked to actively move their fingers following the sphere indicator and the ghost hand.

The experiment consisted of one familiarization cycle and five regular cycles. The familiarization cycle was included to allow the participants to practice the procedure and was not recorded. Each cycle contained one perception-test trial, two control trials, and 18 viscosity trials (six per viscosity). During the perception-test trial, high viscosity rendering ($\mathrm{B}_3$) was provided to confirm the haptic rendering was correctly working. Then, the control conditions followed, including one passive and one active trial in random order. For the viscosity trials, the six trials per three viscosity levels were presented in random order. Each trial lasted six seconds and covered three complete opening and closing hand movements. For each trial, a $5\,\mathrm{s}$ countdown was displayed on the screen before the beginning. If the trial was the control condition, the condition name and instruction were also shown. "Start" appeared at the trial's beginning and "Stop!" at its end. We included rest periods between trials of $10\,\mathrm{s}$ to $15\,\mathrm{s}$. Additionally, a longer rest period of $30\,\mathrm{s}$ was enforced every five to eight trials. The duration and time when the rest periods were enforced varied to reduce anticipation and keep participants focused. Participants were instructed to avoid blinking or unnecessary movements during the countdown and trial periods.

After the experiment was completed, participants filled in a questionnaire using the Qualtrics XM survey tool (Qualtrics, USA). The first section included the raw Task Load Index (raw-TLX) [19], while the second section asked participants to what extent they could feel different levels of haptic rendering and how many distinct levels they perceived. The total duration of the experiment was around two hours.

### D. EEG Analysis

EEG processing and analysis were conducted with EEGLAB v2024.0 [26] on MATLAB R2021a (MathWorks) and MNE 1.5.1 [27], [28] in Python 3.9.19. As for preprocessing, EEG recordings were downsampled to $256\,\mathrm{Hz}$ before applying a bandpass filter from $1\,\mathrm{Hz}$ to $45\,\mathrm{Hz}$. A low-pass filter was applied before downsampling, which is a built-in process of the MNE package to prevent aliasing. Bad channels were interpolated using the spline method. The EEG was re-referenced to the average reference, and epochs were extracted from two seconds before the trials started until their end. Bad epochs with extreme values or fluctuations were removed using criteria based on Iwane et al.'s work [29]. Preconditioned independent component analysis (ICA) for real data (Picard) was performed on the joined epochs of each participant. Using the independent component (IC) labeling model mne_icalabel [30], [31] and manual inspection, ICs suspected to be eye or muscle artifacts were removed, and the cleaned data was reconstructed using the rest of the ICs.

After preprocessing, time-frequency representation (TFR) was computed for each participant in each condition using the Morlet wavelet transform with a $1\,\mathrm{Hz}$ frequency resolution, covering $1\,\mathrm{Hz}$ to $40\,\mathrm{Hz}$. To quantify the changes in power, we applied the Z-score baseline corrections to the TFR, which involved subtracting the baseline mean and subsequently dividing by the baseline's standard deviation to obtain the result. The baseline recording we used for each condition was the rest period 2 seconds before the trial started.

Initially, a round of cluster-based permutation tests (CBPT) with 1000 permutations was performed on the combined TFRs of all conditions. The combined adjacency matrix used here was calculated on the channels, frequencies, and time points. The one-tailed F-test was used, with a cluster threshold set to the critical F-value for a significance level of 0.05. Significant clusters were identified with a p-value threshold of 0.05.

Next, CBPT with 1000 permutations was conducted on paired conditions using the same adjacency matrix. The two-tailed t-test was employed, with a cluster threshold at the critical t-value for a 0.05 significance level. The Bonferroni correction adjusted the p-value threshold for significant clusters to 0.005, accounting for 10 paired comparisons. These tests were also applied to two pre-selected regions of interest (ROIs) with the same time range (during tasks) and electrodes over the ipsilateral somatosensory cortex ('C2', 'C4', 'C6', 'CCP2h', 'CCP4h', 'CCP6h', 'CP2', 'CP4', 'CP6', 'P2', 'P4', 'P6'). The ROIs differed by frequency: one in the mu-band (8–$13\,\mathrm{Hz}$) and the other in the beta-band (15–$30\,\mathrm{Hz}$).

### E. Behavioral Data and Questionnaires

During the experiment, the system logged data for each time frame, including the timestamp, experimental condition, current and desired finger flexion/extension angular position, finger velocity, and force delivered to the fingers from the device.

The force rendered due to viscosity varies with velocity. Therefore, to check that we performed a fair comparison of EEG data between conditions, we first averaged the velocity and commanded force profiles over the $6\,\mathrm{s}$ trials for each participant and condition, then computed the mean and standard deviations of these averaged profiles across all participants. We also calculated each participant's average tracking error, i.e., the difference between desired and actual finger angular position per condition, and pooled these for group comparisons.

We evaluated differences in tracking error between conditions using a one-way ANOVA. Data normality and variance homogeneity were verified using Shapiro–Wilk and Levene's tests. If the ANOVA was significant, we performed post hoc analysis with Tukey's HSD correction. The significance threshold was set to $\alpha = 0.05$.

Regarding the questionnaire data, we calculated the median, first quartile (Q1), and third quartile (Q3) for each subscale of the raw-TLX questionnaire. We also summarized the extent and number of perceived intensities reported by participants.

## III. Results

### A. EEG Processing

On average, $3.67 \pm 2.67$ (mean $\pm$ standard deviation) epochs were removed per participant from a total of 100. For the subsequent ICA, $2.25 \pm 0.97$ ICs were removed per participant.

We selected two electrodes over the somatosensory cortex, CP3 (left hemisphere) and CP4 (right hemisphere). The group-level Event-Related Spectral Perturbation (ERSP) with Z-score baseline is shown in Fig. 2A, where a clear mu-ERD is evident on both hemispheres after task onset. The group-level mu and beta ERD during hand movement on CP3 and CP4 under different conditions are shown in Fig. 2B.

### B. Cluster-Based Permutation Tests

The CBPT conducted on the full data range across all conditions revealed one significant cluster ($p = 0.001$, the lowest possible p-value with 1000 permutations). To visualize this 3D cluster, we averaged the F-values across all channels and obtained Fig. 3A. A topographic map summarizing the probability of occurrence across time and frequencies is shown in Fig. 3B. These results indicate a significant difference in ERSP among conditions.

Paired tests between the passive and active control conditions did not result in significant clusters. However, we found one significant positive cluster when comparing the passive control condition to each viscosity condition (all $p = 0.001$) and when comparing the active control condition to each viscosity condition (all $p = 0.001$).

For the mu-band ROI, one significant positive cluster was found for each pair that compared the passive control condition with the middle ($p = 0.001$) and high ($p = 0.001$) viscosity conditions, as well as the pairs that compared the active control condition with the low ($p = 0.003$), middle ($p = 0.001$), and high ($p = 0.002$) viscosity conditions. No significant cluster was found in comparisons between the three viscosity conditions or between the control conditions.

For the beta-band ROI, one significant positive cluster was found for each pair that compared the passive control condition with the low ($p = 0.003$), middle ($p = 0.001$), and high ($p = 0.002$) viscosity conditions, as well as the pairs that compared the active control condition with the low ($p = 0.001$), middle ($p = 0.001$), and high ($p = 0.001$) viscosity conditions. No significant cluster was found in the tests between the three viscosity conditions or between the control conditions.

### C. Behavioral Data

For observational comparison proposes, the finger flexion/extension velocities and the forces applied to the fingers by the haptic device over time are plotted in Fig. 4, with their average and standard deviation. Positive forces in the viscosity conditions depict resistance while squeezing the virtual liquid dispenser. The negative forces during the passive control condition depict the assistance to close the hand, while the positive forces are a result of the assistance to open the hand. Ideally, the rendered forces during the active control condition would be constant at $0\,\mathrm{N}$; the positive fluctuations that can be observed originate from the soft-wall constraint protecting participants and the haptic device when approaching the safe operating limit.

The ANOVA test revealed significant differences in the tracking error among the conditions ($F = 13.22$ and $p < 0.001$). In particular, we found the tracking error of the active control condition is significantly higher than the low viscosity condition by $5.01^\circ$ (the difference in means between the two groups, $p < 0.001$), than the middle viscosity condition by $5.28^\circ$ ($p < 0.001$), and than the high viscosity condition by $4.25^\circ$ ($p < 0.001$). Meanwhile, the tracking error of the passive control condition is significantly higher than the low viscosity condition by $2.87^\circ$ ($p < 0.05$) and than the middle viscosity conditions by $3.14^\circ$ ($p < 0.01$).

### D. Task Demand and Perceived Haptic Feedback

The overall raw-TLX subscale scores (0–100) among conditions and participants were as follows: Mental demand (median: 27, Q1: 18, Q3: 33); Physical demand (median: 17, Q1: 6.5, Q3: 37); Temporal demand (median: 17, Q1: 1, Q3: 28.25); Performance (median: 80.5, Q1: 78.5, Q3: 86.25); The effort required (median: 24, Q1: 14, Q3: 37.5); Frustration levels (median: 5.5, Q1: 0.75, Q3: 15.75). According to Hertzum [32], scores below 35 indicate low demand, while scores above 56 indicate high demand. In most cases, our task resulted in reported low demands (mentally, physically, and temporally), with low confusion levels and high performance expectations.

After the experiment, nine out of 12 participants reported "definitely yes" when asked if they could feel different levels of haptic rendering, while two responded "probably yes," and one reported "might or might not." None chose "probably not" or

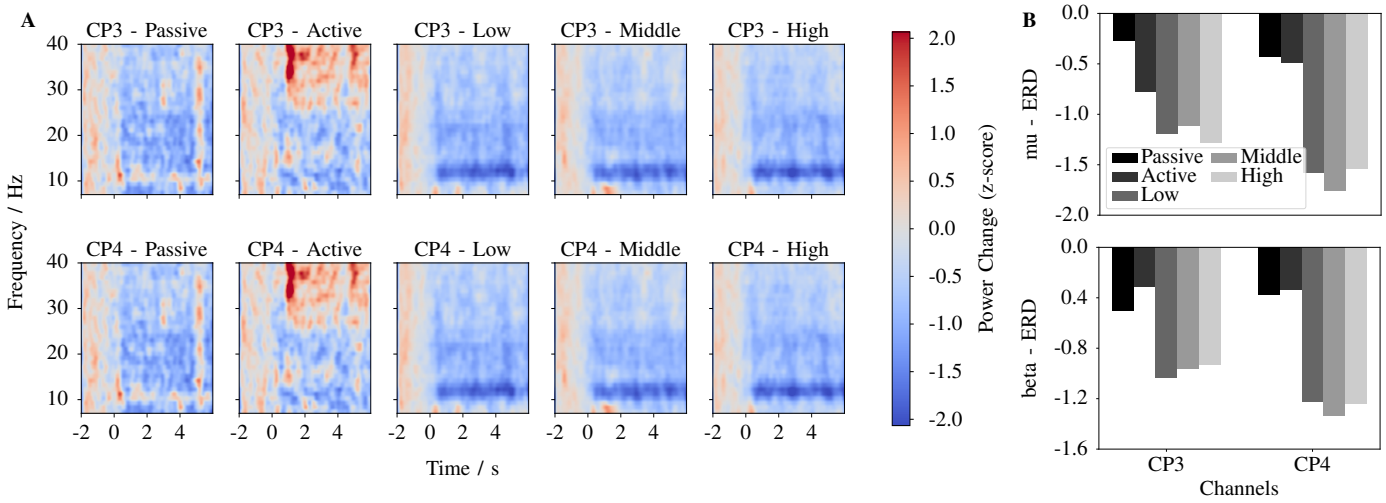


Fig. 2. The group-level ERSP and ERD plots for CP3 and CP4 under all five conditions. (A) The ERSP plot (1–40 Hz) spans two seconds before the trial to its end, showing a clear mu-ERD. (B) The mu-ERD and beta-ERD for all five conditions during hand movement, averaged across all trials.

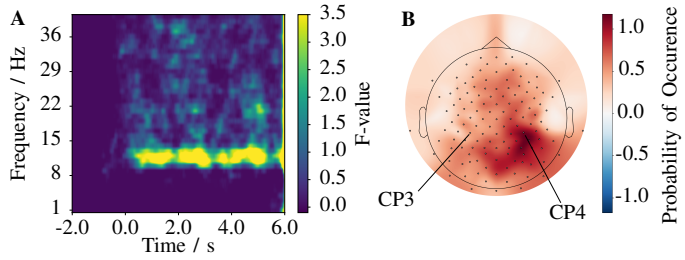


Fig. 3. The significant cluster of the CBPT on the full data range across all conditions. (A) TFR of the significant cluster, averaged over the electrode dimension. (B) Topographic map of the significant cluster averaged over time and frequency dimensions.

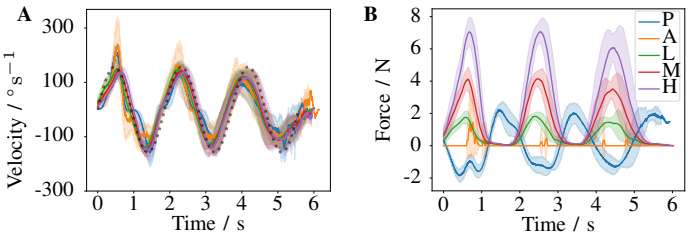


Fig. 4. Mean and standard deviation of the finger flexion/extension velocity (A) and commanded force (B) during a 6 s trial for each condition across all trials and participants (see Section II-E). A trial included three openings and closings of the hand. The dotted line in (A) represents the target velocity profile. In both subplots, P denotes the passive control condition; A represents the active control condition; L, M, and H mean the low, middle, and high viscosity conditions, respectively.

"definitely not." Regarding distinct haptic rendering levels, five participants reported experiencing three levels, three reported four levels, and four reported five levels.

## IV. Discussion

### *A. Viscosity and Stiffness Rendering Relate to Stronger Mu and Beta ERD in the Ipsilateral Somatosensory Cortex*

From the result of CBPT, we observed that both mu-ERD and beta-ERD in the ipsilateral somatosensory cortex were significantly stronger when viscosity and stiffness rendering were present, compared to active movement without haptic rendering or passive movement, except the mu-ERD when comparing the low viscosity condition with the passive movement. These findings align with our first hypothesis, suggesting that incorporating proprioceptive feedback in the form of forces applied to muscles and joints elicits a higher brain response than movement and position proprioception alone.

Previous studies have demonstrated that transcallosal inhibitory interactions, reflected in the ipsilateral sensorimotor cortex as mu-ERD and beta-ERD, can suppress unintended movements of the contralateral stationary limb [33], [34]. These inhibitory mechanisms can also be involved in motor control of the active limb, as evidenced by a positive correlation between ipsilateral cortical activation and hand movement speed [35]. The enhanced ipsilateral cortical activity observed in our conditions featuring stiffness and viscosity rendering aligns with this view, providing further support for the role of ipsilateral activation in the control of the moving hand.

Our findings also reveal that regions with significant mu-ERD and beta-ERD differences were concentrated in the ipsilateral somatosensory cortex. In the contralateral somatosensory cortex, strong ERD activity was observed under all conditions, but the intensity differences between conditions were less pronounced. While the precise neural mechanisms underlying contralateral mu- and beta-band oscillations in sensorimotor tasks are not yet fully understood, these results are consistent with the findings in previous work [29], [36], suggesting that contralateral sensorimotor activation may reach a saturation level.

Although we gave the same movement instruction for all conditions, we observed that the average tracking errors were significantly lower under viscosity conditions than control conditions. The difference in tracking error may also affect our results, since the ERD can also reflect the motor execution process, and lower tracking errors may indicate an easier execution process that requires less mental effort.

### B. No Significant Evidence Was Found that Rendering Higher Viscosity Leads to Stronger ERD

Most participants reported perceiving differences in feedback intensity according to our questionnaire, and the differences in the applied forces during the different viscosity conditions are also evident in Fig. 4B. Moreover, the raw-TLX questionnaire suggests that our experiments involve low task demands, which mitigate the influence of high workload on performance and proprioceptive sensation [20], [21]. Yet, our EEG analysis revealed no significant difference in brain activity across viscosities, rejecting our second hypothesis. This aligns with studies using fixed loads to modulate proprioceptive sensation, which reported that applying different loads during sensorimotor tasks does not significantly affect mu, beta, or gamma band activity in the sensorimotor cortex [12]–[14]. Therefore, we suspect the information about the proprioceptive sensation level may be encoded in deeper brain structures, such as the cerebellum, basal ganglia, and deeper layers of the primary motor cortex, which EEG can hardly capture. We suggest further study on this using fMRI or other modalities with better depth resolution.

However, our results do not align with those from Nakayashiki et al., who found increased mu-ERD in the somatosensory cortex with higher grasping forces [15]. This discrepancy could stem from differences in the experimental designs. Their study focused on a stationary grasping task, primarily involving static force perception, whereas our dynamic squeezing task involved movement. Such movement may have heightened proprioceptive input and elevated the sensory baseline, potentially obscuring significant variations in mu-ERD. Similarly, Ortega et al. found no correlation between grip force and mu-ERD averaged over the trial. However, they observed a negative correlation between the force and mu-band signal intensity during the onset phase [37]. We did not observe differences at the movement onset, probably because our experiment included a five-second countdown that allowed participants to anticipate the task, potentially mitigating mu-band desynchronization during the onset phase. This may indicate that the mu rhythm plays a role in perception preparation. Additionally, since the beta rhythm is known to be involved in movement preparation [38], it is unsurprising that neither Ortega et al. nor we found significant differences in beta-ERD during the onset phase. In both studies, movement patterns remained consistent within each experiment, minimizing perception differences and likely contributing to the observed stability in beta-ERD during the onset phase.

### C. No Significant Difference Was Found between Active and Passive Control Conditions

The CBPT across the full data range revealed no significant difference between passive and active control conditions when haptic rendering was not provided. Similarly, Qiu et al. reported no significant difference in beta-ERD strength between active and passive lower limb movements, despite differences in characteristic frequencies [39]. Keinrath et al. also found no significant difference in mu-ERD strength during active and passive upper limb movements [40]. These findings suggest that mu-ERD and beta-ERD are insensitive to motor intention but reflect proprioceptive sensations from movements, whether self-initiated or externally applied.

Formaggio et al. similarly observed ERD similarities between active and passive hand movements but noted pre-movement alpha synchronization (in the mu-band frequency range) during active movement only [41]. In our experiment, we did not capture this pre-movement difference. Also, there was no advance notice of the upcoming movement in Formaggio et al.'s experiment. Therefore, we still speculate that this phenomenon is caused by perceptual preparation.

### D. Limitations and Future Work

In our experimental design, participants entered the rest periods immediately after completing each trial. Consequently, the EEG signal for each epoch was truncated immediately after the task, preventing analysis of post-movement components such as mu rebound, beta rebound, and prolonged ERD. Future experiments should include instructions to remain still for a few seconds post-task to capture these components. Additionally, the control conditions included fewer trials than the viscosity conditions, and the control conditions were always presented first, potentially reducing the signal-to-noise ratio and introducing order effects. Increasing the number of trials in control conditions and interspersing them between the viscosity conditions would enhance data quality and reduce order effects. Further, the number of participants and the homogeneity of the cohort limit the statistical power and generalizability of the results. Specifically, all participants were young and unimpaired university students, which differs from the intended target group of individuals with ABI. This limits ecological validity, and the results may not fully carry over to clinical populations. Regarding EEG processing, analysis in this study was limited to the channel level due to time and computational constraints. While channel-level analysis remains common in related studies, the crosstalk phenomenon may prevent channel signals from fully reflecting underlying brain activity [42]. Future studies should incorporate source localization methods when feasible to improve accuracy.

## V. Conclusion

In this study, we investigated changes in EEG activity during active grasping movements with fixed stiffness and different viscosity levels. We also evaluated the differences between active movement without haptic rendering and passive movement. We observed that the presence of viscosity and stiffness rendering led to stronger mu-ERD and beta-ERD in the ipsilateral somatosensory cortex during movement, although no significant difference was found between different viscosity levels. Additionally, no significant difference was observed between the passive movement and the active movement without haptic rendering. These findings suggest that the existence of proprioceptive feedback caused by viscosity and stiffness rendering has a potential enhancing effect on somatosensory cortex activity, highlighting its importance in rehabilitation.

## REFERENCES


[1] J. M. Veerbeek, A. C. Langbroek-Amersfoort, E. E. H. van Wegen, C. G. M. Meskers, and G. Kwakkel, "Effects of robot-assisted therapy for the upper limb after stroke," *Neurorehabilitation and Neural Repair*, vol. 31, pp. 107–121, 2 2017. [Online]. Available: http://journals.sagepub.com/doi/10.1177/1545968316666957

[2] J. Mehrholz, A. Pollock, M. Pohl, J. Kugler, and B. Elsner, "Systematic review with network meta-analysis of randomized controlled trials of robotic-assisted arm training for improving activities of daily living and upper limb function after stroke," *Journal of NeuroEngineering and Rehabilitation*, vol. 17, pp. 1–14, 6 2020. [Online]. Available: https://jneuroengrehab.biomedcentral.com/articles/10.1186/s12984-020-00715-0

[3] L. Marchal-Crespo and D. J. Reinkensmeyer, "Review of control strategies for robotic movement training after neurologic injury," *Journal of neuroengineering and rehabilitation*, vol. 6, pp. 1–15, 2009.

[4] J. M. Veerbeek, A. C. Langbroek-Amersfoort, E. E. Van Wegen, C. G. Meskers, and G. Kwakkel, "Effects of robot-assisted therapy for the upper limb after stroke: a systematic review and meta-analysis," *Neurorehabilitation and neural repair*, vol. 31, no. 2, pp. 107–121, 2017.

[5] R. Gassert and V. Dietz, "Rehabilitation robots for the treatment of sensorimotor deficits: a neurophysiological perspective," *Journal of neuroengineering and rehabilitation*, vol. 15, pp. 1–15, 2018.

[6] Z. Zhang and D. Sternad, "Back to reality: differences in learning strategy in a simplified virtual and a real throwing task," *Journal of Neurophysiology*, vol. 125, no. 1, pp. 43–62, 2021.

[7] J. C. Metzger, O. Lambercy, A. Califfi, D. Dinacci, C. Petrillo, P. Rossi, F. M. Conti, and R. Gassert, "Assessment-driven selection and adaptation of exercise difficulty in robot-assisted therapy: A pilot study with a hand rehabilitation robot," *Journal of NeuroEngineering and Rehabilitation*, vol. 11, no. 1, pp. 1–14, 2014.

[8] K. Salisbury, F. Conti, and F. Barbagli, "Haptic rendering: introductory concepts," *IEEE computer graphics and applications*, vol. 24, no. 2, pp. 24–32, 2004.

[9] R. Rätz, F. Conti, I. Thaler, R. M. Müri, and L. Marchal-Crespo, "Enhancing stroke rehabilitation with whole-hand haptic rendering: development and clinical usability evaluation of a novel upper-limb rehabilitation device," *Journal of neuroengineering and rehabilitation*, vol. 21, no. 1, p. 172, 2024. [Online]. Available: https://doi.org/10.1186/s12984-024-01439-1

[10] S. Hussain, P. K. Jamwal, P. V. Vliet, and N. A. T. Brown, "Robot assisted ankle neuro-rehabilitation: State of the art and future challenges," *Expert Review of Neurotherapeutics*, vol. 21, pp. 111–121, 1 2021. [Online]. Available: https://www.tandfonline.com/doi/full/10.1080/14737175.2021.1847646

[11] A. Bodegård, S. Geyer, P. Herath, C. Grefkes, K. Zilles, and P. E. Roland, "Somatosensory areas engaged during discrimination of steady pressure, spring strength, and kinesthesia," *Human Brain Mapping*, vol. 20, no. 2, pp. 103–115, 10 2003. [Online]. Available: https://doi.org/10.1002/hbm.10125

[12] Y. Wang, L. Cao, D. Hao, Y. Rong, L. Yang, S. Zhang, F. Chen, and D. Zheng, "Effects of force load, muscle fatigue and extremely low frequency magnetic stimulation on EEG signals during side arm lateral raise task," *Physiological Measurement*, vol. 38, no. 5, pp. 745–758, 4 2017.

[13] K. Nakayashiki, M. Saeki, Y. Takata, Y. Hayashi, and T. Kondo, "Modulation of event-related desynchronization during kinematic and kinetic hand movements," *Journal of NeuroEngineering and Rehabilitation*, vol. 11, no. 1, p. 90, 2014.

[14] V. Chakarov, J. R. Naranjo, J. Schulte-Mönting, W. Omlor, F. Huethe, and R. Kristeva, "Beta-range EEG-EMG coherence with isometric compensation for increasing modulated low-level forces," *Journal of Neurophysiology*, vol. 102, no. 2, pp. 1115–1120, 8 2009.

[15] K. Nakayashiki, H. Tojiki, Y. Hayashi, S. Yano, and T. Kondo, "Brain Processes Involved in Motor Planning Are a Dominant Factor for Inducing Event-Related Desynchronization," *Frontiers in Human Neuroscience*, vol. 15, 11 2021.

[16] J. L. Emken and D. J. Reinkensmeyer, "Robot-enhanced motor learning: accelerating internal model formation during locomotion by transient dynamic amplification," *IEEE Transactions on Neural Systems and Rehabilitation Engineering*, vol. 13, no. 1, pp. 33–39, 2005.

[17] Y. Abdel Majeed, S. Awadalla, and J. L. Patton, "Effects of robot viscous forces on arm movements in chronic stroke survivors: a randomized crossover study," *Journal of NeuroEngineering and Rehabilitation*, vol. 17, pp. 1–9, 2020.

[18] R. Shadmehr and F. A. Mussa-Ivaldi, "Adaptive representation of dynamics during learning of a motor task," *Journal of neuroscience*, vol. 14, no. 5, pp. 3208–3224, 1994.

[19] S. G. Hart, "NASA-task load index (NASA-TLX); 20 years later," in *Proceedings of the Human Factors and Ergonomics Society*, vol. 50, no. 9. Sage publications Sage CA: Los Angeles, CA, 2006, pp. 904–908.

[20] F. Ribeiro and J. Oliveir, "Factors Influencing Proprioception: What do They Reveal?" in *Biomechanics in Applications*. chapter, 2011, vol. 14.

[21] K. Yasuda, Y. Sato, N. Iimura, and H. Iwata, "Allocation of Attentional Resources toward a Secondary Cognitive Task Leads to Compromised Ankle Proprioceptive Performance in Healthy Young Adults," *Rehabilitation Research and Practice*, vol. 2014, pp. 1–7, 2014.

[22] R. Rätz, F. Conti, R. M. Müri, and L. Marchal-Crespo, "A Novel Clinical-Driven Design for Robotic Hand Rehabilitation: Combining Sensory Training, Effortless Setup, and Large Range of Motion in a Palmar Device," *Frontiers in Neurorobotics*, vol. 15, no. December, pp. 1–22, 2021.

[23] R. Rätz and L. Marchal-Crespo, "Physics Engine-Based Whole-Hand Haptic Rendering for Sensorimotor Neurorehabilitation," *2023 IEEE World Haptics Conference, WHC 2023 - Proceedings*, pp. 279–285, 2023.

[24] M. Scandola, M. Vicentini, and P. Fiorini, "How force perception changes in different refresh rate conditions," in *IEEE 15th International Conference on Advanced Robotics: New Boundaries for Robotics, ICAR 2011*, 2011, pp. 322–327. [Online]. Available: http://www.safros.eu

[25] M. Scandola, M. Vicentini, L. Gasperotti, D. Zerbato, and P. Fiorini, "Force feedback in psychophysics research: even low performance algorithms may lead to realistic perceptual experience," in *Proceedings of the 27th Annual Meeting of the International Society for Psychophysics*, 2011.

[26] A. Delorme and S. Makeig, "EEGLAB: An open source toolbox for analysis of single-trial EEG dynamics including independent component analysis," *Journal of Neuroscience Methods*, vol. 134, no. 1, pp. 9–21, 3 2004.

[27] E. Larson, A. Gramfort, D. A. Engemann, J. Leppakangas, C. Brodbeck, M. Jas *et al.*, "MNE-Python," 2023. [Online]. Available: https://doi.org/10.5281/zenodo.8322569

[28] A. Gramfort, A. Luessi, E. Larson, D. A. Engemann, D. Strohmeier, C. Brodbeck *et al.*, "MEG and EEG data analysis with MNE-Python," *Frontiers in Neuroscience*, no. 7 DEC, 2013.

[29] F. Iwane, G. Lisi, and J. Morimoto, "EEG sensorimotor correlates of speed during forearm passive movements," *IEEE Transactions on Neural Systems and Rehabilitation Engineering*, vol. 27, no. 9, pp. 1667–1675, 9 2019.

[30] A. Li, J. Feitelberg, A. P. Saini, R. Höchenberger, and M. Scheltienne, "Mne-icalabel: Automatically annotating ica components with iclabel in python," *Journal of Open Source Software*, vol. 7, no. 76, p. 4484, Aug. 2022. [Online]. Available: http://dx.doi.org/10.21105/joss.04484

[31] L. Pion-Tonachini, K. Kreutz-Delgado, and S. Makeig, "Iclabel: An automated electroencephalographic independent component classifier, dataset, and website," *NeuroImage*, vol. 198, p. 181–197, Sep. 2019. [Online]. Available: http://dx.doi.org/10.1016/j.neuroimage.2019.05.026

[32] M. Hertzum, "Reference values and subscale patterns for the task load index (TLX): a meta-analytic review," *Ergonomics*, vol. 64, no. 7, pp. 869–878, 2021.

[33] D. T. Bundy and E. C. Leuthardt, "The cortical physiology of ipsilateral limb movements," *Trends in neurosciences*, vol. 42, no. 11, pp. 825–839, 2019.

[34] V. Beaulé, S. Tremblay, and H. Théoret, "Interhemispheric control of unilateral movement," *Neural plasticity*, vol. 2012, no. 1, p. 627816, 2012.

[35] T. Tazoe and M. A. Perez, "Speed-dependent contribution of callosal pathways to ipsilateral movements," *Journal of Neuroscience*, vol. 33, no. 41, pp. 16 178–16 188, 2013.

[36] J. Barone and H. E. Rossiter, "Understanding the role of sensorimotor beta oscillations," *Frontiers in Systems Neuroscience*, vol. 15, p. 655886, 2021.

[37] P. Ortega, T. Zhao, and A. A. Faisal, "HYGRIP: Full-Stack Characterization of Neurobehavioral Signals (fNIRS, EEG, EMG, Force, and Breathing) During a Bimanual Grip Force Control Task," *Frontiers in Neuroscience*, vol. 14, 10 2020.

[38] M. Hervault, P. G. Zanone, J. C. Buisson, and R. Huys, "Cortical sensorimotor activity in the execution and suppression of discrete and rhythmic movements," *Scientific Reports*, vol. 11, no. 1, 12 2021.

[39] S. Qiu, W. Yi, J. Xu, H. Qi, J. Du, C. Wang, F. He, and D. Ming, "Event-Related Beta EEG Changes during Active, Passive Movement and Functional Electrical Stimulation of the Lower Limb," *IEEE Transactions on Neural Systems and Rehabilitation Engineering*, vol. 24, no. 2, pp. 283–290, 2 2016.

[40] C. Keinrath, S. Wriessnegger, G. R. Müller-Putz, and G. Pfurtscheller, "Post-movement beta synchronization after kinesthetic illusion, active and passive movements," *International Journal of Psychophysiology*, vol. 62, no. 2, pp. 321–327, 11 2006.

[41] E. Formaggio, S. F. Storti, I. Boscolo Galazzo, M. Gandolfi, C. Geroin, N. Smania, A. Fiaschi, and P. Manganotti, "Time–Frequency Modulation of ERD and EEG Coherence in Robot-Assisted Hand Performance," *Brain Topography*, vol. 28, no. 2, pp. 352–363, 3 2015.

[42] F. D. Putri and V. Nadhira, "Quantitative EEG Based on Direct Recording and Source Localization Estimation in Repetitive Hand Motor Activity," *International Journal Bioautomation*, vol. 27, no. 1, p. 51, 2023.